AAV2/9-mediated overexpression of MIF inhibits SOD1 misfolding, delays disease onset, and extends survival in mouse models of ALS

Marcel F. Leyton-Jaimes[a,b], Joy Kahn[a,b], and Adrian Israelson[a,b,1]

[a]Department of Physiology and Cell Biology, Faculty of Health Sciences, Ben-Gurion University of the Negev, Beer Sheva 84105, Israel; and [b]The Zlotowski Center for Neuroscience, Ben-Gurion University of the Negev, Beer Sheva 84105, Israel

Edited by Lawrence Steinman, Stanford University School of Medicine, Stanford, CA, and approved June 4, 2019 (received for review March 21, 2019)

Mutations in superoxide dismutase (SOD1) cause amyotrophic lateral sclerosis (ALS), a neurodegenerative disease characterized by the loss of upper and lower motor neurons. Transgenic mice that overexpress mutant SOD1 develop paralysis and accumulate misfolded SOD1 onto the cytoplasmic faces of intracellular organelles, including mitochondria and endoplasmic reticulum (ER). Recently, macrophage migration inhibitory factor (MIF) was shown to directly inhibit mutant SOD1 misfolding and binding to intracellular membranes. In addition, complete elimination of endogenous MIF accelerated disease onset and late disease progression, as well as shortened the lifespan of mutant SOD1 mice with higher amounts of misfolded SOD1 detected within the spinal cord. Based on these findings, we used adeno-associated viral (AAV) vectors to overexpress MIF in the spinal cord of mutant SOD1^{G93A} and loxSOD1^{G37R} mice. Our data show that MIF mRNA and protein levels were increased in the spinal cords of AAV2/9-MIF–injected mice. Furthermore, mutant SOD1^{G93A} and loxSOD1^{G37R} mice injected with AAV2/9-MIF demonstrated a significant delay in disease onset and prolonged survival compared with their AAV2/9-GFP–injected or noninjected littermates. Moreover, these mice accumulated reduced amounts of misfolded SOD1 in their spinal cords, with no observed effect on glial overactivation as a result of MIF up-regulation. Our findings indicate that MIF plays a significant role in SOD1 folding and misfolding mechanisms and strengthen the hypothesis that MIF acts as a chaperone for misfolded SOD1 in vivo and may have further implications regarding the therapeutic potential role of up-regulation of MIF in modulating the specific accumulation of misfolded SOD1.

ALS | mutant SOD1 | misfolded SOD1 | MIF | AAV

Amyotrophic lateral sclerosis (ALS) is a fast progressive neurodegenerative disease caused by the selective loss of upper and lower motor neurons in the brain and spinal cord. Most cases of ALS are sporadic and lack any apparent genetic linkage, but 10% of the cases are dominantly inherited ("familial ALS," fALS) (1). The second most common cause of these familial cases (~20%) is attributed to mutations in a gene encoding for the ubiquitous cytoplasmic copper/zinc superoxide dismutase (SOD1) (2), and overexpression of mutant SOD1 in mouse models of ALS has always resulted in the loss of motor neurons and progressive paralysis (3). Although the mechanisms underlying SOD1-mediated toxicity are still not fully understood, many of the pathways that were proposed to cause motor neuron degeneration in ALS involve damage that is incurred by the accumulation of misfolded SOD1 (4), as determined by using antibodies that bind preferentially to epitopes on misfolded conformers (5–7).

The accumulation of misfolded proteins in spinal motor neurons is a hallmark of both familial and sporadic ALS (8) and has been demonstrated in different model systems (9–14) showing that the misfolded protein may mediate its toxic effects via a variety of mechanisms. Among these being the formation of protein aggregates, supported by the presence of ubiquitinated insoluble inclusions in both familial and sporadic ALS cases that are SOD1 immunoreactive (15, 16), thus suggesting that the systems responsible for maintaining protein homeostasis and preventing protein aggregation are compromised not only in familial but also in sporadic ALS patients (17). Specifically, the accumulation of misfolded SOD1 in sporadic ALS patients has been reported by several groups (15, 18–24), although others have reached the opposite conclusion (25–28).

Additionally, misfolded SOD1 toxicity may be attributed to its association with the mitochondria (10, 29–33) and/or endoplasmic reticulum (ER) (34–37), specifically in tissues from the nervous system. This association of mutant SOD1 with the ER has been implicated in the induction of ER stress (34–37), and misfolded SOD1 was found in fractions enriched for mitochondria derived from ALS-affected tissues, but not from unaffected ones (29, 30, 32, 33, 38, 39). In addition, misfolded SOD1, in its nonaggregated, soluble form, has been found deposited on the cytoplasmic face of the outer membrane of spinal cord mitochondria (30, 32), and this deposition was accompanied by altered mitochondrial shape and distribution (39). These phenomena may be caused, at least in part, by binding of misfolded SOD1 directly to the mitochondrial voltage-dependent anion channel-1 (VDAC1), as such binding inhibits the ability of VDAC1 to transfer adenine nucleotides across the outer mitochondrial membrane (10). Another possible cause is an interaction between misfolded SOD1 and other components in the outer mitochondrial membrane, including Bcl-2 (40) and the protein import machinery (41).

The molecular determinants that underlie the selective accumulation and binding of misfolded mutant SOD1 to the spinal cord mitochondria and ER are still unknown. We have recently found a key modifier of mutant SOD1 misfolding, namely macrophage

Significance

ALS can be caused by mutations in SOD1, which lead to the accumulation of misfolded SOD1 proteins and to the death of motor neurons. Here, we show that elevating MIF levels in the spinal cord can suppress misfolded SOD1 accumulation and aggregation and extend survival of mutant SOD1 mice. This study thus sheds light on the important implications of modulating MIF levels and provides insights regarding the potential therapeutic role of MIF in suppressing the selective accumulation of misfolded SOD1 in ALS.

Author contributions: M.F.L.-J. and A.I. designed research; M.F.L.-J. and J.K. performed research; M.F.L.-J., J.K., and A.I. analyzed data; and J.K. and A.I. wrote the paper.

The authors declare no conflict of interest.

This article is a PNAS Direct Submission.

[1]To whom correspondence may be addressed. Email: adriani@bgu.ac.il.

This article contains supporting information online at www.pnas.org/lookup/suppl/doi:10.1073/pnas.1904665116/-/DCSupplemental.

Published online July 1, 2019.

migration inhibitory factor (MIF). MIF is a homotrimer, which has been implicated in both extracellular and intracellular functions and is synthesized as a cytoplasmic protein (11, 42). MIF acts as a cytokine (43) and was also shown to have chaperone-like activity (44) and thiol oxidoreductase activity (45), in addition to a tautomerase activity (46). We have shown that MIF acts as a cytosolic chaperone that inhibits mutant SOD1 misfolding onto the mitochondria and ER, with MIF levels being extremely low within the cytosol of motor neurons (11). Importantly, we have recently demonstrated that MIF catalytic activities are not required for its protective function as a chaperone (47).

Moreover, we reported that overexpressing MIF in primary motor neurons and neuronal cultures suppresses the accumulation of misfolded SOD1 and rescues them from mutant SOD1-induced cell death (11, 13). In contrast, completely eliminating MIF significantly enhances the accumulation of misfolded SOD1 and its association with mitochondria and ER membranes, ultimately accelerating disease onset and decreasing the survival of the SOD1^{G85R} mice (13).

In the current study, we used adeno-associated virus (AAV) to enhance MIF levels in the spinal cord of the transgenic mutant SOD1^{G93A} and loxSOD1^{G37R} mice as a means to determine how elevating MIF levels in the central nervous system affects the disease course as well as the accumulation and localization of misfolded SOD1.

Results

The Transduction Pattern and Persistence of AAV2/9 In Vitro and In Vivo. To test the ability of AAV2/9-GFP and AAV2/9-MIF virions (Fig. 1*A*) to infect neurons in vitro, we first infected primary motor neurons isolated from mouse embryo spinal cords. Ten days postinfection, the cells were harvested, the motor neuron extract was run on SDS/PAGE, and the levels of MIF and GFP were analyzed by immunoblot. MIF levels were strongly up-regulated in AAV2/9-MIF infected motor neurons compared with noninfected or AAV2/9-GFP infected ones (Fig. 1*B*). We next examined the infection efficacy of our virions on primary hippocampal neurons. As can be clearly observed by immunofluorescence analysis, AAV2/9-MIF infected neurons strongly express MIF compared with AAV2/9-GFP infected neurons (Fig. 1*C*). Since the virions were shown to be effective in vitro, we next evaluated the in vivo infection efficiency in wild type as well as SOD1^{G93A} mice, which develop a rapid and fatal motor neuron disease (48). The SOD1^{G93A} mice were injected intraspinally at postnatal day 1 (to be referred to as P1) (*SI Appendix*, Fig. S1) with 1.26×10^7 vg of self-complementary AAV2/9-expressing GFP from the cytomegalovirus (CMV) enhancer/β-actin promoter (AAV2/9-GFP; $n = 3$ per group). Four weeks postinjection, the animals were killed and spinal cord sections were examined for GFP expression by confocal microscopy (Fig. 1*D*). Transduction efficiency was high in the ventral and dorsal horns of the lumbar spinal cord on both sides. Moreover, we determined the transduction efficiency of AAV2/9-MIF viral particles in vivo by immunoblot (Fig. 1*E*) and quantitative real-time PCR (Fig. 1 *F* and *G*). The data show that MIF protein levels were higher in the spinal cord of AAV2/9-MIF–injected mice compared with AAV2/9-GFP–injected ones (Fig. 1*E*). Furthermore, quantitative real-time PCR monitored 30 d postinjection revealed significantly higher levels of MIF mRNA in the spinal cords of AAV2/9-MIF–injected SOD1^{G93A} (Fig. 1*F*, blue) and loxSOD1^{G37R} (Fig. 1*G*, blue) mice compared with the AAV2/9-GFP controls (Fig. 1 *F* and *G*, red).

Delayed Onset and Extended Survival of SOD1^{G93A} Mice Injected with AAV2/9-MIF. Disease onset (measured by weight loss from denervation-induced muscle atrophy) was significantly delayed by a median of 13 d for SOD1^{G93A} mice injected with AAV2/9-MIF compared with the SOD1^{G93A} littermates injected with AAV2/9-GFP

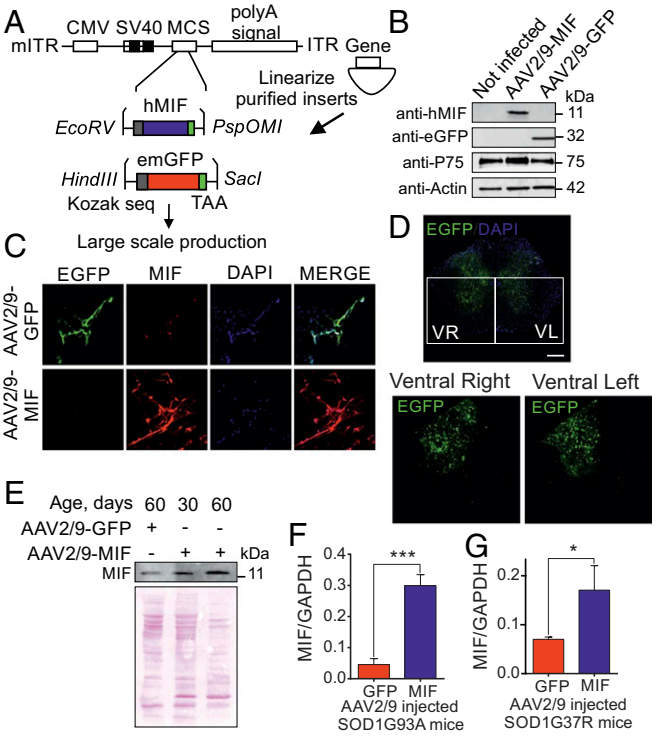

Fig. 1. AAV2/9 vector shows efficient transduction of MIF protein in vitro and in vivo. (*A*) AAV2/9-MIF and AAV2/9-GFP vector design is shown. (*B*) Virion particles (AAV2/9-MIF and AAV2/9-GFP) were evaluated for infectivity by immunoblot in primary motor neurons using anti-MIF and anti-EGFP antibodies. Anti-p75 was used as a motor neuron marker and anti-actin as a loading control. (*C*) Confocal imaging of immunocytochemistry analysis of hippocampal neurons infected with AAV2/9-GFP (green) and AAV2/9-MIF (red). DAPI in blue was used for nuclear staining. (*D*) Confocal imaging of immunohistochemistry analysis of lumbar spinal cord sections of 1-mo-old mice injected at P1 with AAV2/9-GFP (green). DAPI in blue was used for nuclear staining. (Scale bar: 50 μm.) (*E*) Two microliters of AAV2/9-MIF virions were intraspinally injected into P1 mice that were killed 1 or 2 mo postinjection to determine the efficiency and long-lasting effects of AAV2/9-MIF expression. Immunoblot analysis was performed using anti-MIF antibody and ponceau staining is shown as a loading control. (Scale bar: 200 μm.) (*F* and *G*) RNA isolated from the spinal cords of AAV2/9-GFP (red) or AAV2/9-MIF (blue) injected SOD1^{G93A} (*F*) or loxSOD1^{G37R} (*G*) mice was used to analyze MIF levels by quantitative reverse-transcriptase PCR. RNA collected from AAV2/9-MIF–injected animals had an increase of 6 and 2.5 folds in MIF RNA levels in SOD1^{G93A} and loxSOD1^{G37R}, respectively, at the end stage. The bar graph represents mean ± SEM. *P* value was determined by Student's *t* test. ***$P < 0.001$, *$P < 0.05$.

(Fig. 2 *A* and *C*; AAV2/9-GFP: 112 d; AAV2/9-MIF: 125 d; $P < 0.05$). Furthermore, survival of SOD1^{G93A} mice was significantly extended by AAV2/9-MIF injection, yielding median survival time 30 d beyond that of AAV2/9-GFP–injected SOD1^{G93A} mice (AAV2/9-GFP: 148 d; AAV2/9-MIF: 178 d; $P < 0.01$) (Fig. 2 *B* and *E*). Defining disease duration as the time from onset to end stage revealed that the AAV2/9-MIF–treated group had significantly increased duration, indicative of slower disease progression, compared with the AAV2/9-GFP–injected mice (AAV2/9-GFP: 36 d; AAV2/9-MIF: 53 d; $P < 0.01$) (Fig. 2*D*). In addition, AAV2/9-MIF–injected SOD1^{G93A} mice maintained their weight and had better forelimb and hindlimb grip strength test compared with the AAV2/9-GFP age-matched controls (*SI Appendix*, Fig. S2), indicating that AAV2/9-MIF–treated animals maintained their motor function during their prolonged survival. Importantly, a post hoc analysis showed no differences between AAV2/9-GFP and uninjected animals. Moreover, we showed that

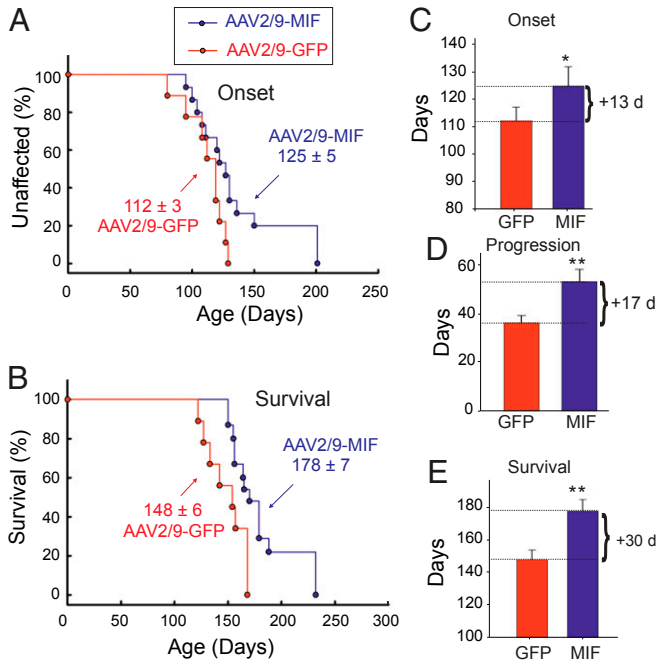

Fig. 2. Overexpression of MIF in the spinal cord delays disease onset and extends the survival of SOD1^{G93A} mice. SOD1^{G93A} mice received a single intraspinal injection of AAV2/9-MIF at P1 ($n = 15$, blue) or AAV2/9-GFP ($n = 9$, red). Treated mice were monitored up to end stage. AAV2/9-MIF injection into P1 SOD1^{G93A} mice significantly delayed median disease onset (*A* and *C*) compared with AAV2/9-GFP–injected mice (AAV2/9-GFP: 112 d; AAV2/9-MIF: 125 d; $P < 0.05$) and extended median disease progression (AAV2/9-GFP: 36 d; AAV2/9-MIF: 53 d; $P < 0.01$) (*D*) and median survival (*B* and *E*) (AAV2/9-GFP: 148 d; AAV2/9-MIF: 178 d; $P < 0.01$). Mean age of disease onset was determined as the time when mice reached peak body weight. Disease progression was defined as the time from onset to end stage. Disease end stage was determined as the time when the mouse could not right itself within 20 s when placed on its side. At each time point, *P* value was determined by *t* test. Error bars denote SEM. $^{**}P < 0.01$; $^{*}P < 0.05$.

AAV2/9-MIF is safe and well tolerated in nontransgenic mice. These AAV2/9-MIF–injected mice showed a steady increase in body mass similar to untreated mice and the weekly behavioral tests revealed no significant defects in motor skills in nontransgenic injected mice as measured by forelimb and hindlimb grip strength (*SI Appendix*, Fig. S2).

Reduction of Misfolded SOD1 Accumulation in the Spinal Cord of AAV2/9-MIF–Treated SOD1^{G93A} Mice. To test the efficacy of AAV2/9-MIF–mediated reduction of misfolded SOD1, we treated cohorts of SOD1^{G93A} mice with a single intraspinal injection of AAV2/9-MIF at P1 (5.35×10^8 vg, $n = 15$). Immunofluorescence with a conformational antibody that specifically recognizes misfolded SOD1, B8H10 (13), was used to determine the accumulation of misfolded SOD1 in end-stage spinal cords of treated and control mice. End-stage mice were perfused with 4% PFA, and frozen sections of spinal cord were stained by free-floating technique with different antibodies. Mutant SOD1^{G93A} mice injected with AAV2/9-MIF had lower accumulation of misfolded SOD1 in the lumbar spinal cord, as observed by the low reactivity to B8H10 (Fig. 3 *E* and *I*), which correlates with higher expression of MIF (Fig. 3 *F* and *J*) compared with that of SOD1^{G93A} mice injected with AAV2/9-GFP (Fig. 3 *A*, *B*, *I*, and *J*). This finding accompanies the extended survival of the mice that were injected with AAV2/9-MIF compared with the AAV2/9-GFP–injected controls (Fig. 2).

AAV2/9-MIF–Mediated Reduction of Misfolded SOD1 Had No Effect on the Overactivation of Astrocytes and Microglia in the SOD1^{G93A} Mice. Noncell autonomous mechanisms play a crucial role in ALS pathology. Specifically, hyperactivation of astrocytes (49) and microglia (50) were shown to drive disease progression in the late phase. Despite the reduction of misfolded SOD1 accumulation in the spinal cords of SOD1^{G93A} mice injected with AAV2/9-MIF (Fig. 3), immunofluorescence imaging of end-stage spinal cords revealed no difference in the number of activated microglia (IbaI staining) (Fig. 4 *A*–*F*) and astrocytes (GFAP staining) (Fig. 4 *G*–*L*) in AAV2/9-MIF–treated animals versus AAV2/9-GFP–injected controls.

AAV9-MIF–Mediated Reduction of Misfolded SOD1 Delayed Onset and Extended Survival in the Slow Progressive loxSOD1^{G37R} Model of ALS. To test the efficacy of AAV2/9-MIF in an additional model of ALS, we treated cohorts of the slow progressive loxSOD1^{G37R} mice (50) with a single intraspinal injection of AAV2/9-MIF or AAV2/9-GFP at P1 as we have done with SOD1^{G93A} mice. In this case, disease onset was significantly delayed by a median of 33 d for loxSOD1^{G37R} mice injected with AAV2/9-MIF compared with their AAV2/9-GFP–injected littermates and 18 d compared with noninjected loxSOD1^{G37R} mice (Fig. 5 *A* and *C*; AAV2/9-GFP: 220 d; noninjected: 235 d; AAV2/9-MIF: 253 d; $P < 0.05$). Survival of loxSOD1^{G37R} mice was significantly extended by AAV2/9-MIF injection, by a median of 27 d compared with

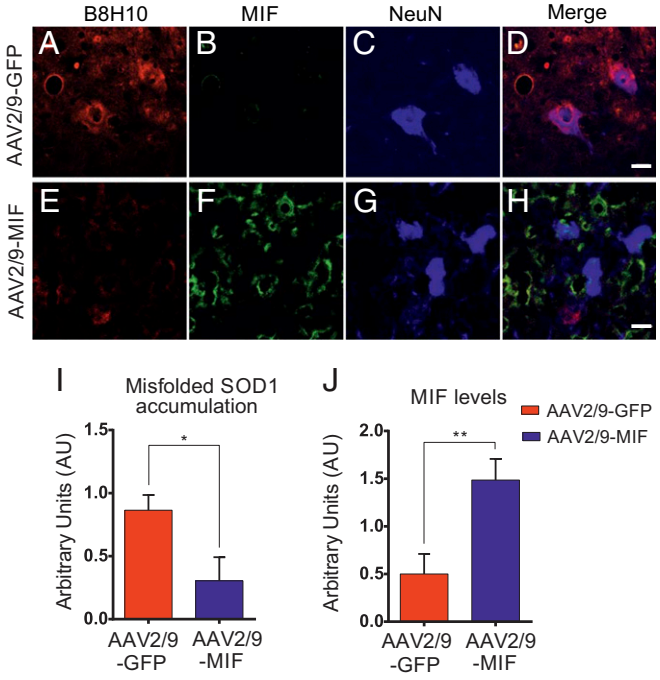

Fig. 3. Overexpression of MIF in the spinal cord suppresses the accumulation of misfolded SOD1 in the SOD1^{G93A} mouse model of ALS. Representative micrographs of lumbar spinal cord sections from AAV2/9-GFP–treated SOD1^{G93A} mice (*A*–*D*) and AAV2/9-MIF–treated SOD1^{G93A} mice (*E*–*H*), processed for immunofluorescence by using the B8H10 antibody, which detects misfolded SOD1 (*A* and *E*), anti-MIF (*B* and *F*), and anti-NeuN antibody, which detects neuronal cells (*C* and *G*). Overexpression of MIF inhibits the accumulation of misfolded SOD1 species as detected by B8H10 antibody. (Scale bar: 25 μm.) (*I* and *J*) Quantification of the relative fluorescence intensity of the B8H10 (*I*) or anti-MIF (*J*) staining of lumbar spinal cord from SOD1^{G93A} mice injected with AAV2/9-GFP (red) or AAV2/9-MIF (blue). About 30 to 35 different areas from different mice of each treatment were analyzed. The bar graph represents mean ± SEM. *P* value was determine by Student's *t* test. $^{**}P < 0.01$; $^{*}P < 0.05$.

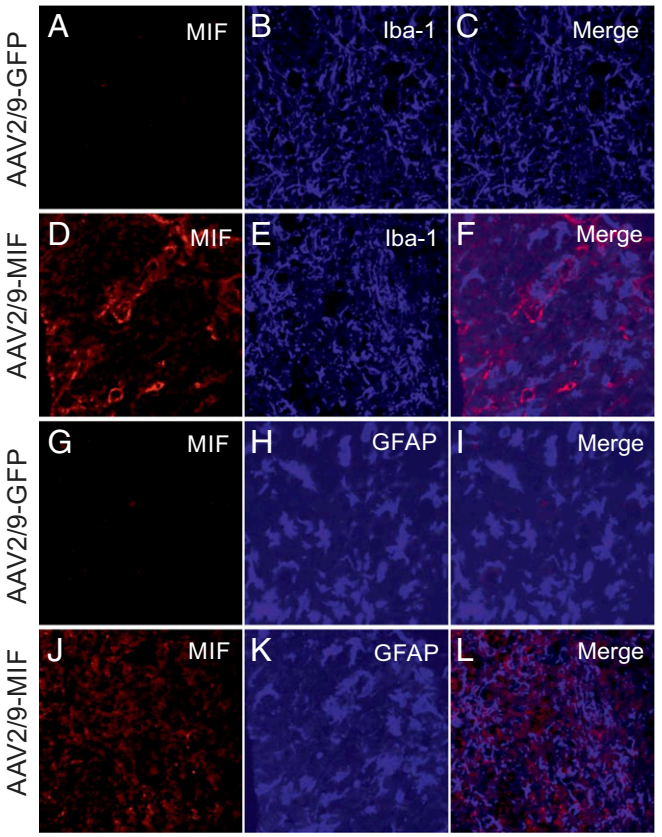

Fig. 4. Overexpression of MIF in the spinal cord does not affect the overactivation of astrocytes and microglia in SOD1^{G93A} mice. Representative micrographs of lumbar spinal cord sections from AAV2/9-GFP–treated SOD1^{G93A} mice (*A–C* and *G–I*) and AAV2/9-MIF–treated SOD1^{G93A} mice (*D–F* and *J–L*), processed for immunofluorescence by using the anti-MIF antibody (*A*, *D*, *G*, and *J*) anti-Iba1 antibody, which detects activated microglia (*B* and *E*) and anti-GFAP, which detects activated astrocytes (*H* and *K*). No significant difference was observed in microglia (*A–F*) or astrocyte (*G–L*) activation following the overexpression of MIF in the spinal cord. (Scale bar: 25 μm.)

AAV2/9-GFP–injected littermates and 22 d compared with noninjected loxSOD1^{G37R} mice (Fig. 5 *B* and *D*; AAV2/9-GFP: 384 d; noninjected: 389 d; AAV2/9-MIF: 411 d; $P < 0.01$). Importantly, the injection of AAV2/9-GFP had no significant effect on disease onset or survival compared with noninjected loxSOD1^{G37R} littermates (Fig. 5). In addition, as we have shown before for SOD1^{G93A} mice, injection of AAV2/9-MIF into the spinal cord of P1 loxSOD1^{G37R} mice strongly reduced the accumulation of misfolded SOD1 in the spinal cord as analyzed by immunostaining with B8H10 antibody (*SI Appendix*, Fig. S3), but had no effect on the overactivation of microglia (*SI Appendix*, Fig. S4).

Discussion

Although the first mutations in SOD1 were found in ALS patients more than 25 y ago, what determines the selective, age-dependent degeneration of upper and lower motor neurons in ALS is still unknown. In mutant SOD1-related ALS cases, motor neuron death is accompanied by the accumulation of misfolded SOD1 and its association with intracellular organelles (10, 11, 13). Moreover, the accumulation of misfolded SOD1 and its mitochondrial association in vitro correlates with the severity of the disease in mutant SOD1 patients (9). A few years ago, we determined that such association of misfolded SOD1 with the mitochondria and ER can be suppressed by a cytosolic protein with chaperone-like activity named MIF, which inhibits SOD1 misfolding (11) and formation of SOD1 amyloid aggregates (47). Moreover, we have shown that MIF levels are extremely low within the motor neuron cell bodies, and that up-regulation of MIF extends the survival of motor neurons and neuronal cell lines (11, 13, 47). Eliminating endogenous MIF in a mutant SOD1 mouse model of ALS accelerated disease onset and progression. Finally, the lack of MIF in motor neurons correlates with higher accumulation of misfolded SOD1 species and mitochondrial association (13).

Notably, it was recently shown that overexpressing the chaperone protein hsp110 in neurons extends the survival of SOD1^{G85R}-YFP and SOD1^{G93A} mice (51). However, altering the expression levels of other chaperones previously linked to SOD1, including hsp70, hsp90, hsp27, and αB-crystallin, failed to significantly affect the disease course in different mutant SOD1 mouse models (52–56).

In the current study, using a gene-targeting approach based on adeno-associated virus AAV2/9, we demonstrate that increasing the expression of the chaperone-like protein, MIF, in vivo in the spinal cord delays disease onset and late disease progression as well as significantly extends the lifespan of two different mutant SOD1 mouse models. Importantly, the delay of disease onset and progression was accompanied by a reduction of misfolded SOD1 accumulation in the spinal cord. However, the overactivation of microglia and astrocytes normally observed at the late stages of the disease, was not affected by MIF overexpression. Our results also show that intraspinal cord injection of AAV2/9-MIF is safe and well tolerated in wild-type mice, without any adverse effects following long term assessment.

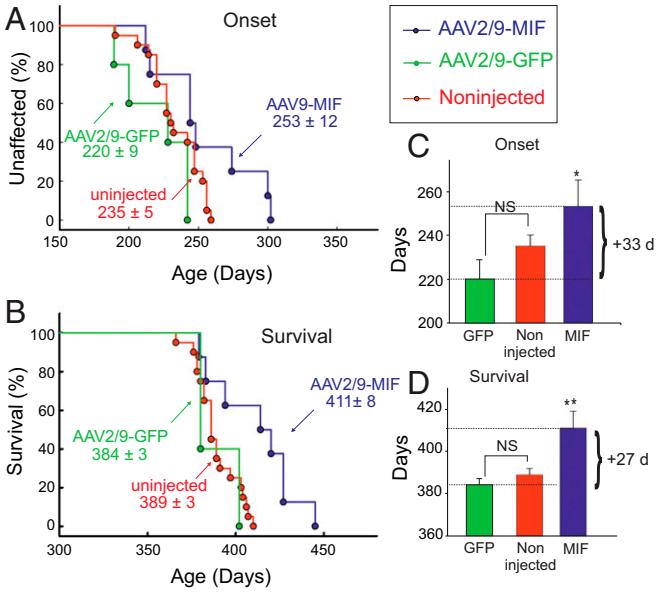

Fig. 5. Overexpression of MIF in the spinal cord delays disease onset and extends the survival of loxSOD1^{G37R} mice. loxSOD1^{G37R} mice received a single intraspinal injection of AAV2/9-MIF at P1 ($n = 8$, blue). Treated mice were monitored up to end stage and compared with AAV2/9-GFP–injected ($n = 5$, green) or noninjected mice ($n = 20$, red). AAV2/9-MIF injection into P1 SOD1^{G37R} mice significantly delayed median disease onset (*A* and *C*) compared with AAV2/9-GFP–injected or to noninjected mice (AAV2/9-GFP: 220 d; noninjected: 235 d; AAV2/9-MIF: 253 d; $P < 0.05$) and extended median survival (*B* and *D*) (AAV2/9-GFP: 384 d; noninjected: 389 d; AAV2/9-MIF: 411 d; $P < 0.01$). Mean age of disease onset was determined as the time when mice reached peak body weight. Disease end stage was determined as the time when the mouse could not right itself within 20 s when placed on its side. At each time point, *P* value was determined by *t* test. Error bars denote SEM. $^{**}P < 0.01$; $^{*}P < 0.05$; NS, no significance.

Apart from MIF's protective function in this context, we must take into consideration the inflammatory effects of MIF when overexpressed in a tissue for long periods (42). For instance, it has been shown that MIF levels increased in microglia located in the epicentral lesion 3 d after spinal cord injury (SCI) in rats (57). This up-regulation of MIF levels correlates with data from human patients suffering from acute (58) or chronic SCI (59).

Moreover, injection of a MIF antagonist peptide into the spinal cord reduces expression of proinflammatory genes and is neuroprotective in a model of encephalomyelitis (60). These data suggest that MIF elicits its pathological functions in the spinal cord by activation of proinflammatory mechanisms which may induce profound neurotoxic effects in the spinal cord (61). Therefore, although such toxic effects were not observed in our studies, a strategy to avoid such potential toxicity will have to be undertaken in the future development of a MIF-based therapy for ALS.

Alongside the question of MIF's therapeutic relevance lies the debate about the AAV approach as a therapeutic gene delivery tool. The small DNA genome of AAV can be successfully replaced with a gene of interest that is packaged into replication-defective viral particles, thus serving as an efficient mechanism for intracellular delivery of the gene of interest. Importantly, AAV vectors do not require integration for gene expression. Usually, expression from these vectors results in extrachromosomal persistence as episomes (62).

In addition to being efficient, AAV-mediated expression is also stable. For example, recombinant AAV expression has been shown to be sustained 15 y in the primate brain (63) and up to 19 mo in the rat brain with no obvious side effects (64). In dog studies, long-term gene expression has been noted for up to 8 y, which represents almost the lifespan of the dog (65). In human trials, the longest follow-up has been reported in patients with hemophilia B, and durability appears to be good at up to 10 y (66). Encouragingly, the US Food and Drug Administration (FDA) has recently approved the first AAV gene therapy treatment for inherited retinal disease (IRD) and many other AAV clinical trials are currently underway, including trials for neurodegenerative diseases. In patients with spinal muscular atrophy (SMA1), a single i.v. infusion of AAV vector encoding SMN resulted in longer survival, superior achievement of motor milestones, and better motor function than in historical cohorts. This treatment can increase serum aminotransferase (a liver enzyme) levels to a degree that is considered a serious adverse event. However, this can be controlled with steroid medication treatment (67).

Therefore, recombinant AAV may serve as a very attractive therapeutic delivery tool in general and in the nervous system in particular, especially since wild-type AAV is known to be nonpathogenic.

Undoubtedly, safety issues will remain the main goal in the field. Therefore, many aspects of AAV biology, such as immunogenicity and potential genotoxicity will have to be further elucidated. Although animal models remain essential for the development of optimized gene therapy drugs, in some cases, only human studies will definitely determine the real therapeutic value of these strategies.

Further supporting AAV studies in the CNS in general, and strengthening our current findings in particular, are recently published gene-targeting studies using AAV9. Using AAV9-shRNA for silencing mutant SOD1 increased survival of $SOD1^{G93A}$ mice by 38% when injected at P1 (68). In addition, overexpressing the neurotrophic factor neuroregulin by intramuscular injection enhanced muscle reinnervation but was not enough for improving the global disease outcome of the $SOD1^{G93A}$ mice (69). Finally, overexpressing IGF1 in the spinal cord by AAV9 administration increased median survival of mutant SOD1 mice by only 7% (70).

Taken together, we propose that MIF chaperone-like activity in the spinal cord may play a crucial role for suppressing the accumulation of misfolded SOD1 and its subsequent toxicity, as we have previously proposed (13), thus overexpressing MIF in the spinal cord may have future therapeutic significance in the treatment of ALS. Furthermore, given the critical involvement of MIF in processes related to misfolding and neurodegeneration, as reported here and before (11, 13, 42, 47), it will be interesting to test whether MIF can function as a protein modifier in other familial-related cases of ALS, FTD, and other neurological diseases such as Alzheimer's, Parkinson's, or Huntington's diseases in which misfolded proteins play a central role.

In summary, the identification of MIF as a cytosolic chaperone-like protein that modifies misfolded SOD1 and possibly inhibits its aggregation in vivo suggests avenues for therapies in ALS, mediated by increasing intracellular MIF levels within the nervous system.

Materials and Methods

SOD1 Transgenic Mice. Transgenic mice expressing the human $SOD1^{G93A}$ and $loxSOD1^{G37R}$ were as originally described (48, 50). Importantly, all mouse lines were bred on a pure C57BL6 background to eliminate confounding genetic influences. $SOD1^{G93A}$ mice were injected with AAV2/9-MIF ($n = 15$) or AAV2/9-GFP ($n = 9$) to obtain the experimental cohorts that were compared. Similarly, $loxSOD1^{G37R}$ mice were injected with AAV2/9-MIF ($n = 8$) or AAV2/9-GFP ($n = 5$) or noninjected ($n = 20$) to obtain the experimental cohorts that were compared. Mice ($loxSOD1^{G37R}$ and $SOD1^{G93A}$) were weighed twice a week as an objective and unbiased measure of disease course (13). Time of disease onset was retrospectively determined as the time when mice reached peak body weight, which is observed before any motor performance decline. Disease end stage was defined by a severe paralysis that the animal could not right itself within 20 s when placed on its side, an endpoint frequently used for mutant SOD1 transgenic mice (13). Mice were genotyped by PCR of DNA extracted from a tail biopsy. All mice were maintained in the animal facility of Ben-Gurion University of the Negev using standard protocols. All procedures involving animals were consistent with the requirements of the Animal Care and Use Committees of Ben-Gurion University of the Negev.

Statistical Analysis. Values are reported throughout as mean ± SEM. Comparisons of two datasets were performed by the Student's t test, after confirming a normal distribution by the Shapiro–Wilk normality test as performed previously (13). Significance was set at a confidence level of 0.05. In all figures, * denotes $P < 0.05$, ** $P < 0.01$, and *** $P < 0.001$. Statistical analysis was performed with SigmaPlot 14 (SYSTAT Software) as previously described (13).

ACKNOWLEDGMENTS. This work was supported by grants from the Israeli Science Foundation (ISF #124/14), FP7 Marie Curie Career Integration Grant (CIG #333794), and The National Institute for Psychobiology in Israel (NIPI #b133-14/15).

1. S. Da Cruz, D. W. Cleveland, Understanding the role of TDP-43 and FUS/TLS in ALS and beyond. *Curr. Opin. Neurobiol.* **21**, 904–919 (2011).
2. D. R. Rosen *et al.*, Mutations in Cu/Zn superoxide dismutase gene are associated with familial amyotrophic lateral sclerosis. *Nature* **362**, 59–62 (1993).
3. B. J. Turner, K. Talbot, Transgenics, toxicity and therapeutics in rodent models of mutant SOD1-mediated familial ALS. *Prog. Neurobiol.* **85**, 94–134 (2008).
4. H. Ilieva, M. Polymenidou, D. W. Cleveland, Non-cell autonomous toxicity in neurodegenerative disorders: ALS and beyond. *J. Cell Biol.* **187**, 761–772 (2009).
5. L. I. Grad *et al.*, Intermolecular transmission of superoxide dismutase 1 misfolding in living cells. *Proc. Natl. Acad. Sci. U.S.A.* **108**, 16398–16403 (2011).
6. F. Gros-Louis, G. Soucy, R. Larivière, J. P. Julien, Intracerebroventricular infusion of monoclonal antibody or its derived fab fragment against misfolded forms of SOD1 mutant delays mortality in a mouse model of ALS. *J. Neurochem.* **113**, 1188–1199 (2010).
7. R. Rakhit *et al.*, An immunological epitope selective for pathological monomer-misfolded SOD1 in ALS. *Nat. Med.* **13**, 754–759 (2007).
8. V. K. Mulligan, A. Chakrabartty, Protein misfolding in the late-onset neurodegenerative diseases: Common themes and the unique case of amyotrophic lateral sclerosis. *Proteins* **81**, 1285–1303 (2013).
9. S. Abu-Hamad, J. Kahn, M. F. Leyton-Jaimes, J. Rosenblatt, A. Israelson, Misfolded SOD1 accumulation and mitochondrial association contribute to the selective vulnerability of motor neurons in familial ALS: Correlation to human disease. *ACS Chem. Neurosci.* **8**, 2225–2234 (2017).

10. A. Israelson *et al*., Misfolded mutant SOD1 directly inhibits VDAC1 conductance in a mouse model of inherited ALS. *Neuron* **67**, 575–587 (2010).
11. A. Israelson *et al*., Macrophage migration inhibitory factor as a chaperone inhibiting accumulation of misfolded SOD1. *Neuron* **86**, 218–232 (2015).
12. C. M. Karch, D. R. Borchelt, Aggregation modulating elements in mutant human superoxide dismutase 1. *Arch. Biochem. Biophys.* **503**, 175–182 (2010).
13. M. F. Leyton-Jaimes *et al*., Endogenous macrophage migration inhibitory factor reduces the accumulation and toxicity of misfolded SOD1 in a mouse model of ALS. *Proc. Natl. Acad. Sci. U.S.A.* **113**, 10198–10203 (2016).
14. M. Prudencio, P. J. Hart, D. R. Borchelt, P. M. Andersen, Variation in aggregation propensities among ALS-associated variants of SOD1: Correlation to human disease. *Hum. Mol. Genet.* **18**, 3217–3226 (2009).
15. K. Forsberg *et al*., Novel antibodies reveal inclusions containing non-native SOD1 in sporadic ALS patients. *PLoS One* **5**, e11552 (2010).
16. T. Ohi, K. Nabeshima, S. Kato, S. Yazawa, S. Takechi, Familial amyotrophic lateral sclerosis with His46Arg mutation in Cu/Zn superoxide dismutase presenting characteristic clinical features and Lewy body-like hyaline inclusions. *J. Neurol. Sci.* **225**, 19–25 (2004).
17. W. E. Balch, R. I. Morimoto, A. Dillin, J. W. Kelly, Adapting proteostasis for disease intervention. *Science* **319**, 916–919 (2008).
18. L. I. Grad *et al*., Intercellular propagated misfolding of wild-type Cu/Zn superoxide dismutase occurs via exosome-dependent and -independent mechanisms. *Proc. Natl. Acad. Sci. U.S.A.* **111**, 3620–3625 (2014).
19. D. A. Bosco *et al*., Wild-type and mutant SOD1 share an aberrant conformation and a common pathogenic pathway in ALS. *Nat. Neurosci.* **13**, 1396–1403 (2010).
20. K. Forsberg, P. M. Andersen, S. L. Marklund, T. Brännström, Glial nuclear aggregates of superoxide dismutase-1 are regularly present in patients with amyotrophic lateral sclerosis. *Acta Neuropathol.* **121**, 623–634 (2011).
21. S. Guareschi *et al*., An over-oxidized form of superoxide dismutase found in sporadic amyotrophic lateral sclerosis with bulbar onset shares a toxic mechanism with mutant SOD1. *Proc. Natl. Acad. Sci. U.S.A.* **109**, 5074–5079 (2012).
22. E. Kabashi, P. N. Valdmanis, P. Dion, G. A. Rouleau, Oxidized/misfolded superoxide dismutase-1: The cause of all amyotrophic lateral sclerosis? *Ann. Neurol.* **62**, 553–559 (2007).
23. E. Pokrishevsky *et al*., Aberrant localization of FUS and TDP43 is associated with misfolding of SOD1 in amyotrophic lateral sclerosis. *PLoS One* **7**, e35050 (2012).
24. P. Zetterström, P. M. Andersen, T. Brännström, S. L. Marklund, Misfolded superoxide dismutase-1 in CSF from amyotrophic lateral sclerosis patients. *J. Neurochem.* **117**, 91–99 (2011).
25. J. I. Ayers *et al*., Conformational specificity of the C4F6 SOD1 antibody; low frequency of reactivity in sporadic ALS cases. *Acta Neuropathol. Commun.* **2**, 55 (2014).
26. S. Da Cruz *et al*., Misfolded SOD1 is not a primary component of sporadic ALS. *Acta Neuropathol.* **134**, 97–111 (2017).
27. A. Kerman *et al*., Amyotrophic lateral sclerosis is a non-amyloid disease in which extensive misfolding of SOD1 is unique to the familial form. *Acta Neuropathol.* **119**, 335–344 (2010).
28. H. N. Liu *et al*., Lack of evidence of monomer/misfolded superoxide dismutase-1 in sporadic amyotrophic lateral sclerosis. *Ann. Neurol.* **66**, 75–80 (2009).
29. H. X. Deng *et al*., Conversion to the amyotrophic lateral sclerosis phenotype is associated with intermolecular linked insoluble aggregates of SOD1 in mitochondria. *Proc. Natl. Acad. Sci. U.S.A.* **103**, 7142–7147 (2006).
30. J. Liu *et al*., Toxicity of familial ALS-linked SOD1 mutants from selective recruitment to spinal mitochondria. *Neuron* **43**, 5–17 (2004).
31. M. Mattiazzi *et al*., Mutated human SOD1 causes dysfunction of oxidative phosphorylation in mitochondria of transgenic mice. *J. Biol. Chem.* **277**, 29626–29633 (2002).
32. C. Vande Velde, T. M. Miller, N. R. Cashman, D. W. Cleveland, Selective association of misfolded ALS-linked mutant SOD1 with the cytoplasmic face of mitochondria. *Proc. Natl. Acad. Sci. U.S.A.* **105**, 4022–4027 (2008).
33. C. Vijayvergiya, M. F. Beal, J. Buck, G. Manfredi, Mutant superoxide dismutase 1 forms aggregates in the brain mitochondrial matrix of amyotrophic lateral sclerosis mice. *J. Neurosci.* **25**, 2463–2470 (2005).
34. A. Mori *et al*., Derlin-1 overexpression ameliorates mutant SOD1-induced endoplasmic reticulum stress by reducing mutant SOD1 accumulation. *Neurochem. Int.* **58**, 344–353 (2011).
35. K. Homma *et al*., SOD1 as a molecular switch for initiating the homeostatic ER stress response under zinc deficiency. *Mol. Cell* **52**, 75–86 (2013).
36. T. Fujisawa *et al*., A novel monoclonal antibody reveals a conformational alteration shared by amyotrophic lateral sclerosis-linked SOD1 mutants. *Ann. Neurol.* **72**, 739–749 (2012).
37. H. Nishitoh *et al*., ALS-linked mutant SOD1 induces ER stress- and ASK1-dependent motor neuron death by targeting Derlin-1. *Genes Dev.* **22**, 1451–1464 (2008).
38. D. Bergemalm *et al*., Overloading of stable and exclusion of unstable human superoxide dismutase-1 variants in mitochondria of murine amyotrophic lateral sclerosis models. *J. Neurosci.* **26**, 4147–4154 (2006).
39. C. Vande Velde *et al*., Misfolded SOD1 associated with motor neuron mitochondria alters mitochondrial shape and distribution prior to clinical onset. *PLoS One* **6**, e22031 (2011).
40. S. Pedrini *et al*., ALS-linked mutant SOD1 damages mitochondria by promoting conformational changes in Bcl-2. *Hum. Mol. Genet.* **19**, 2974–2986 (2010).
41. Q. Li *et al*., ALS-linked mutant superoxide dismutase 1 (SOD1) alters mitochondrial protein composition and decreases protein import. *Proc. Natl. Acad. Sci. U.S.A.* **107**, 21146–21151 (2010).
42. M. F. Leyton-Jaimes, J. Kahn, A. Israelson, Macrophage migration inhibitory factor: A multifaceted cytokine implicated in multiple neurological diseases. *Exp. Neurol.* **301**, 83–91 (2018).
43. M. Merk *et al*., The Golgi-associated protein p115 mediates the secretion of macrophage migration inhibitory factor. *J. Immunol.* **182**, 6896–6906 (2009).
44. O. A. Cherepkova, E. M. Lyutova, T. B. Eronina, B. Y. Gurvits, Chaperone-like activity of macrophage migration inhibitory factor. *Int. J. Biochem. Cell Biol.* **38**, 43–55 (2006).
45. R. Kleemann *et al*., Disulfide analysis reveals a role for macrophage migration inhibitory factor (MIF) as thiol-protein oxidoreductase. *J. Mol. Biol.* **280**, 85–102 (1998).
46. G. Fingerle-Rowson *et al*., A tautomerase-null macrophage migration-inhibitory factor (MIF) gene knock-in mouse model reveals that protein interactions and not enzymatic activity mediate MIF-dependent growth regulation. *Mol. Cell. Biol.* **29**, 1922–1932 (2009).
47. N. Shvil *et al*., MIF inhibits the formation and toxicity of misfolded SOD1 amyloid aggregates: Implications for familial ALS. *Cell Death Dis.* **9**, 107 (2018).
48. M. E. Gurney *et al*., Motor neuron degeneration in mice that express a human Cu,Zn superoxide dismutase mutation. *Science* **264**, 1772–1775 (1994).
49. K. Yamanaka *et al*., Astrocytes as determinants of disease progression in inherited amyotrophic lateral sclerosis. *Nat. Neurosci.* **11**, 251–253 (2008).
50. S. Boillée *et al*., Onset and progression in inherited ALS determined by motor neurons and microglia. *Science* **312**, 1389–1392 (2006).
51. M. Nagy, W. A. Fenton, D. Li, K. Furtak, A. L. Horwich, Extended survival of misfolded G85R SOD1-linked ALS mice by transgenic expression of chaperone Hsp110. *Proc. Natl. Acad. Sci. U S A.* **113**, 5424–5428 (2016).
52. C. M. Karch, D. R. Borchelt, An examination of alpha B-crystallin as a modifier of SOD1 aggregate pathology and toxicity in models of familial amyotrophic lateral sclerosis. *J. Neurochem.* **113**, 1092–1100 (2010).
53. J. Krishnan *et al*., Over-expression of Hsp27 does not influence disease in the mutant SOD1(G93A) mouse model of amyotrophic lateral sclerosis. *J. Neurochem.* **106**, 2170–2183 (2008).
54. J. Liu, L. A. Shinobu, C. M. Ward, D. Young, D. W. Cleveland, Elevation of the Hsp70 chaperone does not effect toxicity in mouse models of familial amyotrophic lateral sclerosis. *J. Neurochem.* **93**, 875–882 (2005).
55. P. S. Sharp *et al*., Protective effects of heat shock protein 27 in a model of ALS occur in the early stages of disease progression. *Neurobiol. Dis.* **30**, 42–55 (2008).
56. G. Xu *et al*., Substantially elevating the levels of αB-crystallin in spinal motor neurons of mutant SOD1 mice does not significantly delay paralysis or attenuate mutant protein aggregation. *J. Neurochem.* **133**, 452–464 (2015).
57. M. Koda *et al*., Up-regulation of macrophage migration-inhibitory factor expression after compression-induced spinal cord injury in rats. *Acta Neuropathol.* **108**, 31–36 (2004).
58. M. Bank *et al*., Elevated circulating levels of the pro-inflammatory cytokine macrophage migration inhibitory factor in individuals with acute spinal cord injury. *Arch. Phys. Med. Rehabil.* **96**, 633–644 (2015).
59. A. Stein *et al*., Pilot study: Elevated circulating levels of the proinflammatory cytokine macrophage migration inhibitory factor in patients with chronic spinal cord injury. *Arch. Phys. Med. Rehabil.* **94**, 1498–1507 (2013).
60. G. Benedek *et al*., HLA-DRα1-mMOG-35-55 treatment of experimental autoimmune encephalomyelitis reduces CNS inflammation, enhances M2 macrophage frequency, and promotes neuroprotection. *J. Neuroinflammation* **12**, 123 (2015).
61. M. Chalimoniuk, K. King-Pospisil, C. N. Metz, M. Toborek, Macrophage migration inhibitory factor induces cell death and decreases neuronal nitric oxide expression in spinal cord neurons. *Neuroscience* **139**, 1117–1128 (2006).
62. D. R. Deyle, D. W. Russell, Adeno-associated virus vector integration. *Curr. Opin. Mol. Ther.* **11**, 442–447 (2009).
63. Y. Sehara *et al*., Persistent expression of dopamine-synthesizing enzymes 15 years after gene transfer in a primate model of Parkinson's disease. *Hum. Gene Ther. Clin. Dev.* **28**, 74–79 (2017).
64. R. J. Mandel *et al*., Recombinant adeno-associated viral vectors as therapeutic agents to treat neurological disorders. *Mol. Ther.* **13**, 463–483 (2006).
65. T. C. Nichols *et al*., Translational data from adeno-associated virus-mediated gene therapy of hemophilia B in dogs. *Hum. Gene Ther. Clin. Dev.* **26**, 5–14 (2015).
66. G. Buchlis *et al*., Factor IX expression in skeletal muscle of a severe hemophilia B patient 10 years after AAV-mediated gene transfer. *Blood* **119**, 3038–3041 (2012).
67. J. R. Mendell *et al*., Single-dose gene-replacement therapy for spinal muscular atrophy. *N. Engl. J. Med.* **377**, 1713–1722 (2017).
68. K. D. Foust *et al*., Therapeutic AAV9-mediated suppression of mutant SOD1 slows disease progression and extends survival in models of inherited ALS. *Mol. Ther.* **21**, 2148–2159 (2013).
69. R. Mancuso *et al*., Neuregulin-1 promotes functional improvement by enhancing collateral sprouting in SOD1(G93A) ALS mice and after partial muscle denervation. *Neurobiol. Dis.* **95**, 168–178 (2016).
70. W. Wang *et al*., Systemic administration of scAAV9-IGF1 extends survival in $SOD1^{G93A}$ ALS mice via inhibiting p38 MAPK and the JNK-mediated apoptosis pathway. *Brain Res. Bull.* **139**, 203–210 (2018).